©Operative Dentistry, 2019, **44-4,** 365-378

Laboratory Research

Effect of Beam Profiles From Different Light Emission Tip Types of Multiwave Light-emitting Diodes on the Curing Profile of Resin-based Composites

DCRS de Oliveira • MG Rocha • AB Correr • JL Ferracane • MAC Sinhoreti

Clinical Relevance

Clinicians should be aware that regardless of the uniformity of the wavelength distribution of beam emissions from multiwave LEDs, violet emittance at 380-420 nm is not capable of being transmitted with depth equivalent to that of blue light.

SUMMARY

Light activation is an important clinical step for achieving success in restorative procedures. This study evaluated the influence of beam profile from different light emission tip types of multiwave light-emitting diodes (LEDs) on the curing profile of resin-based composites. Experimental composites were produced containing either camphorquinone (CQ) or diphenyl(2,4,6-trimethylbenzoyl)phosphine oxide (TPO) as a photoinitiator. Multiwave LEDs with either a bundle light guide tip (Bluephase G2, Ivoclar Vivadent) or a microlens tip (VALO Cordless, Ultradent) were characterized using a beam profiler. Block-shaped samples (5×5×3 mm depth) of the two composites were cured in a custom-designed mold with the multiwave LEDs positioned to compare the regions exposed to the 420-495 nm (blue) and 380-420 nm (violet) emittances. To map the curing profile, the degree of conversion (DC) of longitudinal thin cross sections from each block was evaluated using transmission FT-NIR. Radiant exposure transmitted through the composites during curing was evaluated at different thicknesses. Data were

†Dayane Carvalho Ramos Salles de Oliveira, Department of Restorative Dentistry, Piracicaba Dental School, State University of Campinas, Piracicaba, SP, Brazil

*†Mateus Garcia Rocha, Department of Restorative Dentistry, Piracicaba Dental School, State University of Campinas, Piracicaba, SP, Brazil

Américo Bortolazzo Correr, Department of Restorative Dentistry, Piracicaba Dental School, State University of Campinas, Piracicaba, SP, Brazil

Jack Liborio Ferracane, Department of Restorative Dentistry, School of Dentistry, Oregon Health & Science University, Portland, OR, USA

Mario Alexandre Coelho Sinhoreti, Department of Restorative Dentistry, Piracicaba Dental School, State University of Campinas, Piracicaba, SP, Brazil

*Corresponding author: 901 Limeira Ave, Piracicaba, SP, Brazil, 13414-903; e-mail: grochamateus@gmail.com

†These authors contributed equally to this work.

DOI: http://doi.org/10.2341/16-242

analyzed using analysis of variance and Tukey test (α=0.05; "β=0.2). The results indicated that there were differences in the beam profile and the overall radiant exposures transmitted through the composites using each multiwave LED ($p<0.01$, $df=1$ $F=73.18$). However, there were no differences in the curing profiles provided by the two multiwave LEDs ($p=0.89$, $df=12$ $F=0.52$), and similar effects were found according to the different LED emittance regions ($p=0.09$, $df=5$, $F=2.11$). When considering up to 1 mm in depth, no differences in the DC were found between the composites containing either photoinitiators. Starting at 2 mm in depth, the composite containing TPO showed a decrease in DC in the 420-495 nm emittance region, while the composite containing CQ showed a similar decrease in cure efficiency only at 3-mm depth under both 380-420 nm and 420-495 nm emittance regions. Thus, despite the fact that the nonuniform light beam emitted from the two multiwave LEDs was visually distinctly different when delivering 24 J/cm^2, this difference did not seem to affect the curing profile of the composites. However, light transmission within 380-420 nm seems to be reduced with depth, directly affecting the curing profile of composites containing a photoinitiator with absorbance falling within this emission range.

INTRODUCTION

Light-emitting diodes (LED) are efficient solid-state devices that convert electrical energy directly into visible light (electroluminescence). Incandescent bulbs used in quartz-tungsten-halogen curing lights (QTH) convert about 5% of their power into visible light, while LEDs approach 15% to 20%. Also, QTH light bulbs last from 30 to 50 hours, while LEDs' light emission decays after 100,000 hours of normal use.[1-3]

LEDs, however, have a completely different spectral power distribution, which tends to be narrowband Gaussian with a specific peak and full-width half-maximum of approximately 20 nm.[2,4] The narrowband spectral emission from blue LEDs includes the absorption profile of camphorquinone (CQ) between 420 and 495 nm. However, the activation of alternative photoinitiators having a maximum absorbance in shorter-wavelength ranges creates potential problems.[5,6]

Alternative photoinitiators, such as diphenyl(2,4,6-trimethylbenzoyl)phosphine oxide (TPO), have been suggested as a substitute for CQ in resin materials for esthetic restorations because of the yellow residual color of CQ-based products.[6-8] It should be noted that, despite its yellowing potential, CQ is still present in restorative materials also containing alternative photoinitiators; it is just present in a lowered concentration. Thus, multiwave LEDs are required for photoactivation of the alternative photoinitiators, because their cure efficiency also depends on an absorption in a different wavelength range from CQ.[6]

Multiwave LEDs have developed with a combination of two or more LED chips emitting different wavelength peaks. These combinations provided better cure efficiency for photocurable resin-based materials, regardless of the photoinitiator absorption profile.[9,10] However, the physical location of LED chips in the diode array emitting different wavelengths seems to be associated with the nonuniform nature of the light beam output of these multiwave LEDs.[4,11,12]

Various methods can be used to shape the light beam output from each LED chip, such as microlenses, for example, that are capable of mixing a large portion of a multiwave light beam to give a more uniform beam output,[13] in comparison with optical fiber bundles that can also be used as light guides. Optical fiber bundles can either be coherent or incoherent. Coherent optical fiber bundles have aligned optical fibers from input to output that collimate the output beam without changing the shape of the light output, while incoherent bundles are capable of providing a scrambled light beam output due to the nonaligned optical fibers from the input to output, causing a mixing of the multiwave beam over the tip area.[14] However, no current manufacturer is known to use an incoherent bundle. Thus, the coherent beam emitted reproduces the spatial physical location of the output from individual chips in the LED array. Different output tips are capable of influencing the nonuniform nature of a multiwave beam, and microlenses seems to be a more appropriate system to give a more uniform beam over use of fiber-bundled optics.

The purpose of this study was to evaluate the differences in the beam profiles of two multiwave LEDs having different light emission tip types (microlens or coherent bundle light guide) and to examine the effect of these differences on light transmittance and curing profile of model, resin-based composites containing different photoinitiators (CQ or TPO). The research hypotheses were that 1) the beam profile of multiwave LEDs having different light emission tip types will be visually

Table 1: *Chemical Products Used in Resin-Based Composites Formulation*

Material	Chemical	Concentration, wt%	Manufacturer
Monomer	Bis-GMA	10.15	Sigma Aldrich, St Louis, MO, USA
Monomer	Bis-EMA	11.375	Sigma Aldrich, St Louis, MO, USA
Monomer	UDMA	11.375	Sigma Aldrich, St Louis, MO, USA
Monomer	TEGDMA	2.1	Sigma Aldrich, St Louis, MO, USA
Filler particle	0.05 μm fumed silica	13	Evonik Industries AG, Essen, Germany
Filler particle	0.7 μm $BaBSiO_2$	52	Esstech Inc, Essington, PA, USA

Abbreviations: Bis-GMA, bisphenol A diglycidylmethacrylate; Bis-EMA, ethoxylated bisphenol A diglycidyldimethacrylate; TEGDMA, triethylene glycol dimethacrylate. UDMA, urethane dimethacrylate.

distinctly different and 2) the nonuniform irradiance and wavelengths emitted from multiwave LEDs will significantly reduce the degree of conversion (DC) in areas receiving lower irradiance and in which emissions fall outside of the absorbance range of the photoinitiator system.

METHODS AND MATERIALS

Experimental Resin-Based Composite Formulation

Table 1 lists the monomers and filler particle concentrations used in the experimental resin-based composites. Monomers were blended using a centrifugal mixing device (SpeedMixer, DAC 150.1 FVZ-K, Hauschild Engineering, Hamm, North Rhine-Westphalia, Germany). Equimolar concentrations of either 0.2 wt% CQ (Sigma Aldrich, St Louis, MO, USA) with a tertiary amine (ethyl 4-[dimethylamino]benzoate, EDMAB, Sigma Aldrich; 1:1)[6,15] or 0.4 wt% TPO[6,8] (Sigma Aldrich) were added to the experimental resin. Subsequently, a presilanated fumed silica filler was premixed with the monomer by blending for 30 seconds at 3000 rpm, followed by addition and mixing of a presilanated barium borosilicate glass filler for one minute at 3500 rpm. Then, each resin-based composite was mixed for an additional one minute at 3500 rpm, under vacuum.

Multiwave LED Characterization

The mean irradiance (n=3) from each multiwave LED (Table 2) was evaluated using a portable spectrometer-based instrument (CheckMARC, BlueLight Analytics, Halifax, Nova Scotia, Canada). These values were used to calculate the exposure time needed to produce a minimum radiant exposure of 20 J/cm^2 from each light. Spectral irradiance (mW/cm^2/nm) at the center of each multiwave LED light tip and 2.5 mm toward to the north, south, east, and west directions were also evaluated using a spectrometer (MARC Resin Calibrator, BlueLight Analytics) with a 1-mm diameter aperture over the cosine corrector to selectively measure the spectrum emitted in each region.

As specified by the manufacturer, the Bluephase G2 has four LED chips, one in the violet wavelength range with a spectral emission peak near 410 nm and the other three in the blue wavelength range near 460 nm. The VALO Cordless light, which also has four LED chips, contains one in the violet wavelength range (spectral peak near 405 nm) and the other three in the blue wavelength range, with one chip emitting near 440 nm and two others generating near 460 nm, as illustrated in Figure 1. Thus, the radiant exposure (n=3) over the whole range of violet wavelengths (380-420 nm), over the whole range of blue wavelength (420-495 nm), as well as over the whole ranges of wavelengths of each multiwave LED were calculated by integrating the irradiance vs wavelength curves obtained from a spectrophotometer (MARC Resin Calibrator, BlueLight Analytics) using computer software (Spectra Suite 2.0.140, Ocean Optics, Dunedin, FL, USA).

As shown in Figure 1, the Bluephase G2 and the VALO Cordless units have different light emission tip types to shape their multiwave light beam output. The Bluephase G2 uses a coherent fiber bundle tip, while the VALO Cordless has a quartz microlens. The beam profile of each multiwave curing light was characterized using the beam profiler method.[12-16] Each multiwave LED was attached to an x-y-z positioning device mounted on an optical bench to standardize the positioning of the light beam in contact with a diffusive surface of a frosted diffuser target (DG20-1500, Thorlabs Inc, Newton, NJ, USA), while the resulting image was recorded using a conventional, digital camera (NEX-F3, Sony Corporation, Tokyo, Japan) with a 50-mm focal length lens. Also, to characterize the beam profile of each multiwave curing light through the composite, a 0.5-mm-thick specimen of the resin

Table 2: *Multiwave LEDs Evaluated*

Multiwave LED	Manufacturer	Wavelength Peaks[a]	Irradiance[a]
VALO Cordless (standard mode)	Ultradent, South Jordan, UT, USA	405 nm (violet) 440 nm (blue) 460 nm (blue)	1000 mW/cm^2
Bluephase G2 (high mode)	Ivoclar Vivadent, Schaan, Liechtenstein	410 nm (violet) 460 nm (blue)	1200 mW/cm^2

[a] *According to the manufacturer.*

composite formulation used in the study was used as a screen in substitution of the frosted diffuser target. To assess the irradiance distribution at each of the different LED emission wavelengths from the two multiwave LEDs (as illustrated in Figure 1), the beam profiler was used with the addition of bandpass filters (Thorlabs Inc) placed in front of the camera lens. For the Bluephase G2, a bandpass filter centered first at 400 nm with a 40-nm full width at half maximum (FB400-40) was used to identify the LED chips with spectral emission peaks near 410 nm. A different bandpass filter, centered at 460 nm with a 10-nm full width at half maximum (FB460-10), was used to identify the LED chips generating emission peaks near 460 nm. For the VALO Cordless, the same bandpass filters described above (FB400-40 and FB460-10) were used to identify the LED chips with spectrum emission peaks near 405 nm and 460 nm. An additional bandpass filter, centered at 440 nm with a 10-nm full width at half maximum (FB440-10), was used to identify the LED chip having an emission peak near 440 nm. Because the bandpass filters used in this study have an optical density of approximately 0.2, no neutral-density filters were necessary to attenuate the multiwave LEDs' emission to avoid pixel intensity saturation in the image. To produce calibrated images and data showing the irradiance patterns across the surface of the two multiwave LEDs, the mean power values, obtained using the MARC resin calibrator, were entered into open-source optical analysis software.[17] Because bandpass filters have attenuation loss, the calibration of irradiance values in each image was performed correlating the maximum pixel intensity detected by the camera with the maximum irradiance detected by the spectrophotometer and the total pixel intensity detected by the camera with the total power detected by the spectrophotometer. The scaled numerical data associated with each image was exported into computer graphic software (Origin Pro, OriginLab Co, Northampton, MA, USA).

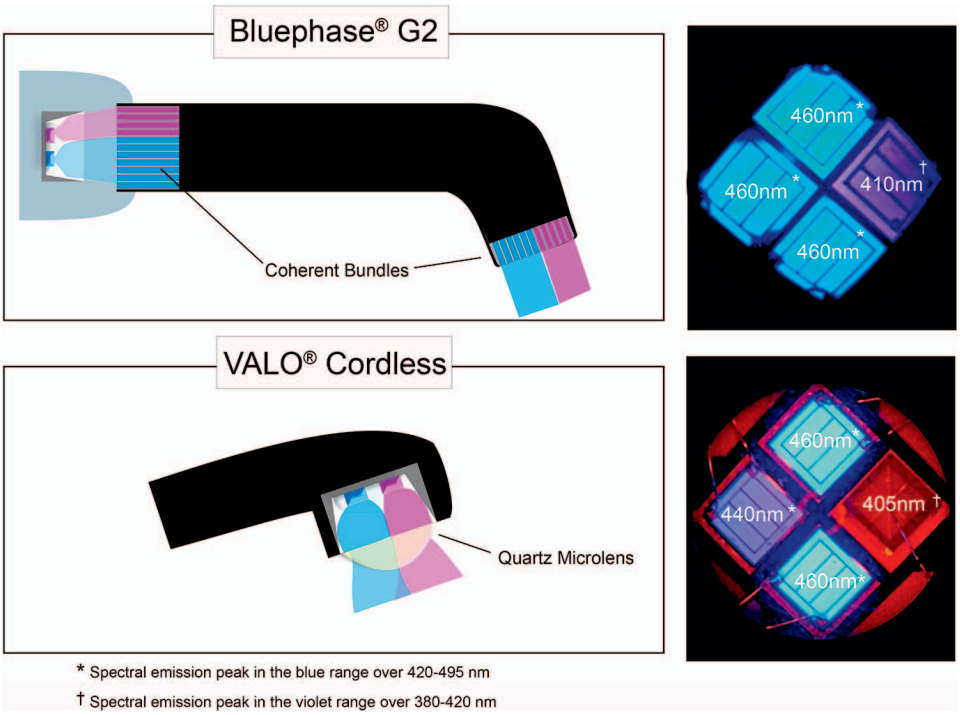

Figure 1. *Schematic distribution of emitted LED wavelengths from the two multiwave LEDs, and actual images of the placement of various wavelength-emitting chips in the light engines of each type curing light.*

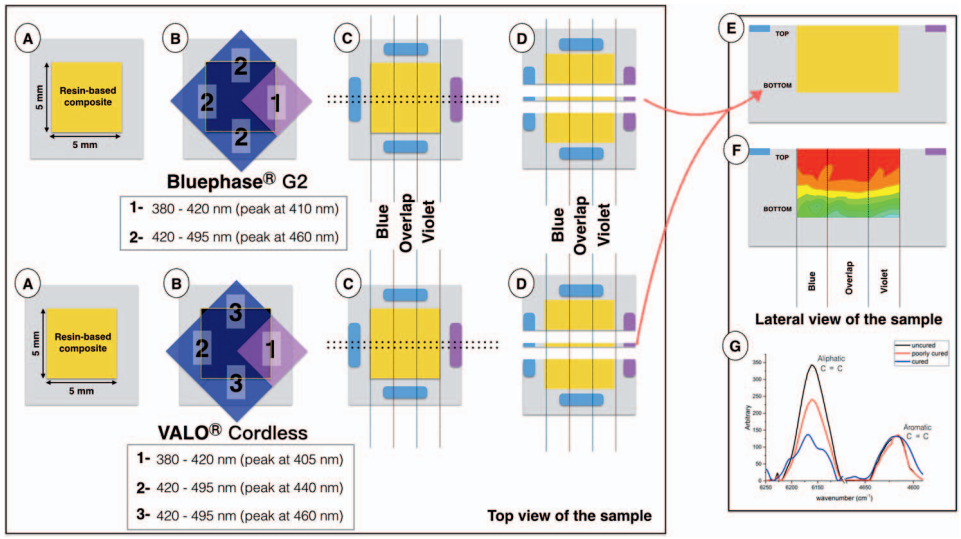

Figure 2. *Schematic design of the experimental setup (A): Resin-based composite (5 mm × 5 mm × 3 mm) placed into the polymethyl methacrylate mold. (B): Light curing using a multiwave LED positioned over the composite specimen. C and D: Dashed lines indicate the cross-section locations (0.5-mm thick) of the center of the block-shaped sample. E and F: Lateral view of a specimen cross section exemplifying the curing profile analysis using transmission FT-NIR microscopy. G: Superimposition of spectral images as examples of the IR absorption profiles depicting uncured, poorly cured, and well-cured resins. The aliphatic, methacrylate C=C absorbs at 6165 cm^{-1} and changes according to polymer curing, while the aromatic C=C absorbance at 4623 cm^{-1} remains stable, despite polymer curing. Higher aliphatic C=C is associated with lower degree of monomer conversion.*

Absorption Spectrophotometric Analysis

Spectrophotometric analysis (n=3) was performed to evaluate the absorption of the photoinitiators in the 200- to 600-nm wavelength range using a UV-Vis spectrophotometer (U-2450, Hitachi High-Technologies, Chiyoda, Tokyo, Japan). Each photoinitiator was diluted in 1 mL of TEGDMA (Sigma-Aldrich). The spectra were collected using a quartz cell with a path length of 1 cm.

Radiant Exposure Transmitted Analysis

Samples of each composite containing the different photoinitiators were prepared using Delrin jigs (Ø=5 mm having 1-, 2-, or 3-mm thickness) placed over the bottom sensor (Ø=3.98 mm) of a spectrophotometer (MARC Resin Calibrator, BlueLight Analytics) with Mylar strips on the top and bottom surfaces. The irradiance between 380-420 nm, 420-495 nm, and over the whole ranges of wavelengths at the bottom of each sample (mW/cm^2) vs time (seconds) of photoactivation with each multiwave LED were recorded during curing (n=3), and the radiant exposure transmitted through each sample (J/cm^2) was obtained from the integration of the irradiance vs time after the recommended radiant exposure to the upper surface had been applied.

Curing Profile Characterization

Block-shaped samples (5×5 mm, 3-mm depth, n=3) were produced by curing each composite in a custom-designed polymethylmethacrylate mold simulating a Class I restoration, as illustrated in Figure 2.[8] The photoactivation using each multiwave LED was performed with the light tip placed directly on the specimen surface with a Mylar strip covering the top. A jig was made to reproducibly position each multiwave LED to establish the regions of the block directly exposed to the 380-420 nm and 420-495 nm LED emittances according to the distribution of each emitted LED wavelength from each multiwave LED.

To map the DC from top to bottom and across the breadth of the block, each block was sectioned, using a water-cooled diamond saw to produce a longitudinal cross section (0.5-mm thick) of the center of each block. An IR thermal camera (FLIR One PRO, FLIR Systems, Wilsonville, OR, USA) was used to live record the overall temperature (°C) increase in the samples during the slicing process. DC was calculated from infrared spectra obtained using an FT-NIR microscope (Nicolet Continuum, Thermo Scientific, Waltham, MA, USA) coupled to an FT-NIR spectrometer (Nicolet Nexus 6700, Thermo Scientific). At every 500 μm in width and depth, an infrared spectrum was collected, resulting in 143 data points for each cross section. Measurements started 300 μm below the top surface to avoid the effects of the oxygen layer inhibition. Spectra were obtained in transmission mode by the coaddition of 64 scans at a resolution of 4 cm^{-1}. FT-NIR readings were performed in the transmission mode rather than the reflection mode to evaluate DC in bulk rather than on the surface of the material, which reduces the influence of monomer elution from the surfaces of section specimens. Vinyl conversion was determined based on the aliphatic absorption band at 6165 cm^{-1},

using the aromatic band at 4623 cm^{-1} as an internal reference. Spectra were collected for the polymerized longitudinal cross-section specimens of each block across the entire length and depth of the cross section and for a nonpolymerized sample of each experimental composite sandwiched between two glass plates (0.5-mm thick). The DC (in %) was calculated as follows[16]:

$$DC(\%) = \left(1 - \frac{Rpol}{Rnonpol}\right) \times 100$$

where R is the ratio of peak areas at 6165 cm^{-1} and 4623 cm^{-1} in polymerized (pol) and nonpolymerized (non pol) specimens.

Monomer conversion results were exported to create color-coded maps to describe DC as a function of position under the light beam using computer graphic software (Origin Pro, OriginLab Co). Each data point registered on the map was the average of three different replications, using similar testing conditions. The map scales were set to indicate the maximum DC achieved and a reduction of 10% of the maximum DC in each subsequent color-coded area.[8]

Statistical Analyses

Data were entered into statistical analysis software (Stata/MP 13, StataCorp, College Station, TX, USA) and passed normality testing (Shapiro-Wilk's test, w=0.79, $p<0.001$) and equivalence of variance homoscedasticity (Levene's test, w50=0.85; Pr>F=0.73). Statistical analyses were performed according to the different experimental designs. A split-plot analysis of variance (ANOVA) was used for the statistical analysis of the curing profile values and a two-way ANOVA for the radiant exposure transmitted values. Tukey's test was applied for multiple comparisons (α=0.05) among the different photoinitiators, LED emittance regions, and depths or thicknesses. Power analysis was conducted to determine the sample size for each experiment to provide a power of at least 0.8 at a significance level of 0.05 ("β=0.2).

RESULTS

Multiwave LED Characterization

The Bluephase G2 had a mean irradiance of 1195 ± 17 mW/cm^2 and a total radiant exposure of 24 ± 0.5 J/cm^2 after 20 seconds of exposure, with 19.4 ± 0.6 J/cm^2 being generated over the blue wavelength range of 420-495 nm and 4.6 ± 0.3 J/cm^2 over the violet wavelength range of 380-420 nm. The VALO Cordless had a mean irradiance of 953 ± 12 mW/cm^2 and a total radiant exposure of 23.8 ± 0.3 J/cm^2 after 25 seconds of exposure (20 seconds of exposure, immediately followed by five more seconds of exposure), with 18.4 ± 0.4 J/cm^2 being contributed over the blue wavelength range of 420-495 nm and 5.4 ± 0.2 J/cm^2 over the violet wavelength range of 380-420 nm. Thus, a standardized radiant exposure of 24 J/cm^2 was used for all photoactivation protocols.

Figure 3 illustrates the spectral irradiance (mW/cm^2/nm) at the center of each multiwave LED light tip and 2.5 mm toward the north, south, east, and west directions. For Bluephase G2, at the center area, a mean irradiance of 452 ± 6.2 mW/cm^2 was detected, with 339 ± 5.1 mW/cm^2 being contributed over the blue wavelength range of 420-495 nm and 113 ± 7.1 mW/cm^2 over the violet wavelength range of 380-420 nm. At the north area, a mean irradiance of 614 ± 5.4 mW/cm^2 was detected, with 489 ± 2.8 mW/cm^2 being contributed over the blue wavelength range of 420-495 nm and 125 ± 9.0 mW/cm^2 over the violet wavelength range of 380-420 nm. At the south area, a mean irradiance of 1336 ± 5.0 mW/cm^2 was detected, with 1269 ± 7.1 mW/cm^2 being contributed over the blue wavelength range of 420-495 nm and 67 ± 3.0 mW/cm^2 over the violet wavelength range of 380-420 nm. At the east area, a mean irradiance of 576 ± 6.4 mW/cm^2 was detected, with 506 ± 3.7 mW/cm^2 being contributed over the blue wavelength range of 420-495 nm and 70 ± 8.9 mW/cm^2 over the violet wavelength range of 380-420 nm. At the west area, a mean irradiance of 831 ± 4.4 mW/cm^2 was detected, with 671 ± 7.7 mW/cm^2 being contributed over the blue wavelength range of 420-495 nm and 160 ± 1.1 mW/cm^2 over the violet wavelength range of 380-420 nm.

For VALO Cordless, at the center area, a mean irradiance of 1315 ± 2.3 mW/cm^2 was detected, with 985 ± 3.0 mW/cm^2 being contributed over the blue wavelength range of 420-495 nm and 330 ± 1.5 mW/cm^2 over the violet wavelength range of 380-420 nm. At the north area, a mean irradiance of 962 ± 3.1 mW/cm^2 was detected, with 784 ± 4.2 mW/cm^2 being contributed over the blue wavelength range of 420-495 nm and 178 ± 1.9 mW/cm^2 over the violet wavelength range of 380-420 nm. At the south area, a mean irradiance of 1374 ± 2.7 mW/cm^2 was detected, with 1061 ± 3.9 mW/cm^2 being contributed over the blue wavelength range of 420-495 nm and 313 ± 1.6 mW/cm^2 over the violet wavelength range of 380-420 nm. At the east area, a mean irradiance of 1453 ± 2.7 mW/cm^2 was detected, with 1145 ± 4.0 mW/cm^2 being contributed over the blue wavelength

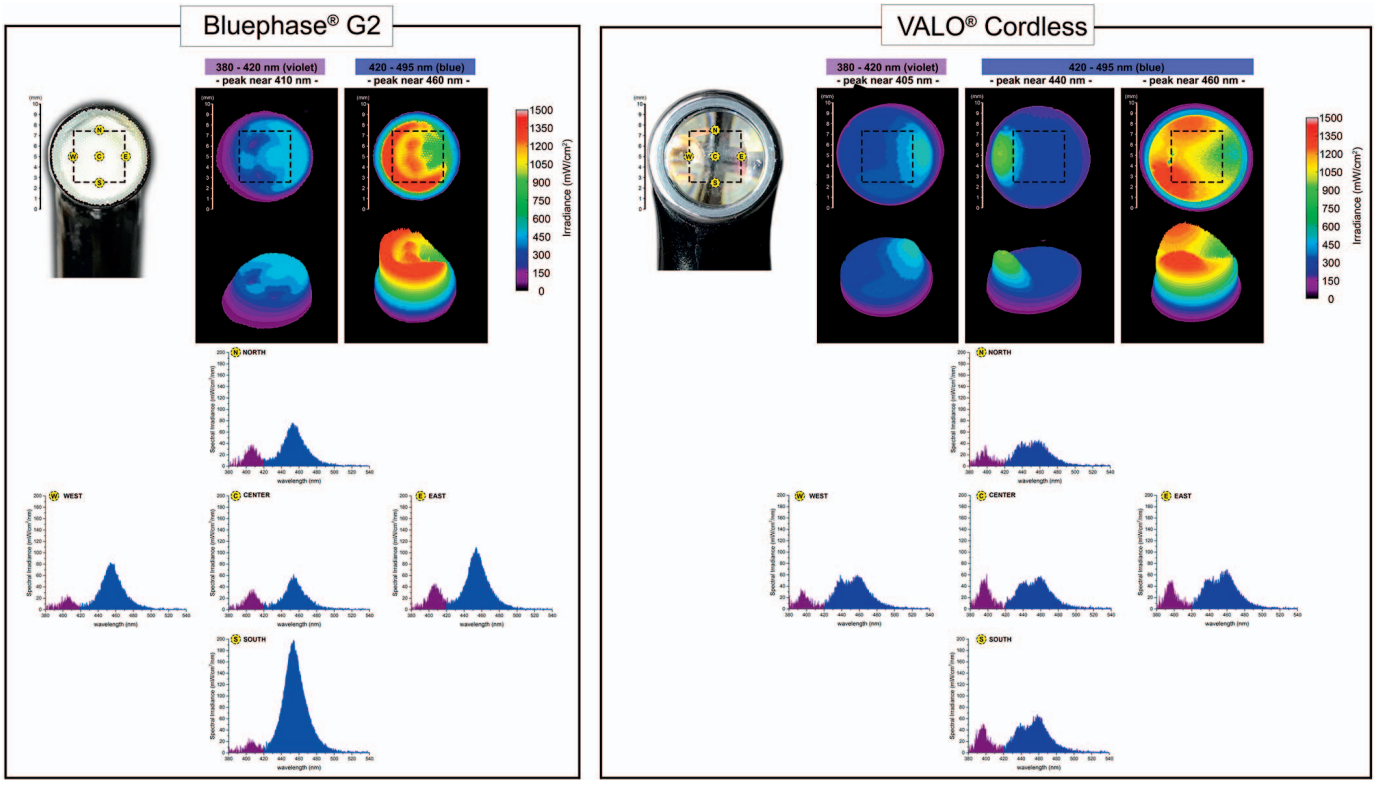

Figure 3. *Beam profile images of the two multiwave LEDs in two dimensions and three dimensions within 420-495 nm (blue) and 380-420 nm (violet) wavelength ranges. The black line outlines where the composite specimen border lies within the beam profile and the spectral irradiance (mW/cm^2/nm) at the center of each multiwave LED light tip and 2.5 mm toward the north, south, west, and east directions.*

range of 420-495 nm and 308 ± 1.4 mW/cm^2 over the violet wavelength range of 380-420 nm. At the west area, a mean irradiance of 1220 ± 3.1 mW/cm^2 was detected, with 1040 ± 3.8 mW/cm^2 being contributed over the blue wavelength range of 420-495 nm and 180 ± 2.4 mW/cm^2 over the violet wavelength range of 380-420 nm.

Also, Figure 3 illustrates the beam profile of the two multiwave LEDs. The Bluephase G2 had an active area of emission of 0.646 cm^2 and a maximum irradiance of 1195 mW/cm^2, but the irradiance and the wavelengths were not uniformly distributed across the tip. For the wavelength emission between 420 and 495 nm, localized standard areas of higher irradiances (1367 mW/cm^2) and lower irradiances (837 mW/cm^2) were seen. For the wavelengths within 380-420 nm, localized areas of higher irradiances (197 mW/cm^2) and lower irradiances (112 mW/cm^2) were observed. The black dashed squares of 5 × 5 mm in Figure 3 represent the area of the light emission tip of each multiwave LED in which the specimens were positioned during photoactivation. Inside the black dashed square area of 5 × 5 mm referenced to the size of the specimen, the Bluephase G2 had an irradiance of 132 mW/cm^2 within 380-420 nm and an irradiance of 756 mW/cm^2 within 420-495 nm.

The VALO Cordless had an active area of emission of 0.750 cm^2 and a maximum irradiance of 953 mW/cm^2, but the irradiance and the wavelengths were not uniformly distributed across the tip. For the wavelength emission between 420 and 495 nm, localized standard areas of higher irradiances (1085 mW/cm^2) and lower irradiances (397.5 mW/cm^2) were seen. For the wavelengths within 380-420 nm, localized areas of higher irradiances (431 mW/cm^2) and lower irradiances (50 mW/cm^2) were seen. Inside the black-lined square area of 5 × 5 mm referenced to the size of the specimen, the VALO Cordless unit had an irradiance of 188 mW/cm^2 within 380-420 nm and irradiance of 864 mW/cm^2 between 420 and 495 nm, whereas 206 mW/cm^2 was generated at 440 nm and 658 mW/cm^2 at 460 nm.

Figure 4 illustrates the beam profile of the two multiwave LEDs through the resin composite used in the study. Inside the black dashed square area of 5 × 5 mm referenced to the size of the specimen, the Bluephase G2 had an irradiance of 140 mW/cm^2 within 380-420 nm and an irradiance of 666 mW/cm^2

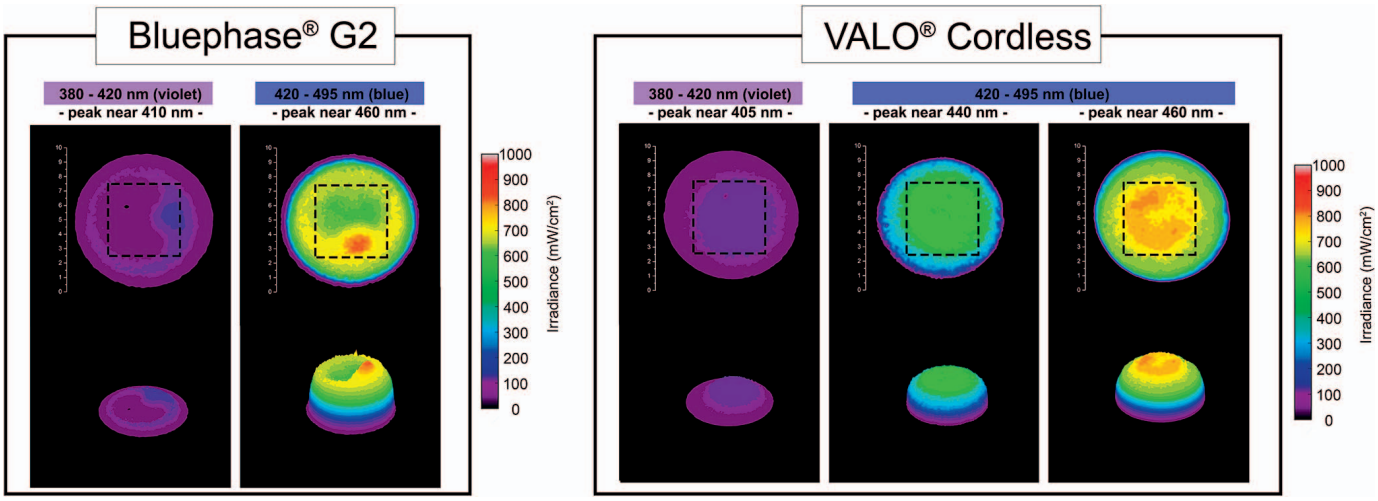

Figure 4. *Beam profile images of the two multiwave LEDs in two dimensions and three dimensions within 420-495 nm (blue) and 380-420 nm (violet) wavelength ranges through the resin composite. The black line outlines where the composite specimen border lies within the beam profile.*

within 420-495 nm; the VALO Cordless unit had an irradiance of 128 mW/cm^2 within 380-420 nm and an irradiance of 640 mW/cm^2 between 420 and 495 nm, whereas 256 mW/cm^2 was generated at 440 nm and 384 mW/cm^2 at 460 nm.

Spectrophotometric Absorption

Figure 5 illustrates the spectral irradiance for the two multiwave LEDs compared with the absorbance of each photoinitiator (CQ and TPO) plotted against the wavelength. As can be observed, the absorption peak of CQ is approximately at 470 nm, which matches the blue light spectrum emission peaks of the multiwave LEDs at 440 nm and 460 nm for the VALO Cordless and 460 nm for the Bluephase G2. Alternatively, the absorption peak of TPO is mainly in the near UV-A region and extends to the violet spectrum range, thus overlapping mostly with the violet light spectrum emission peak of the multiwave LEDs at 405 nm for the VALO Cordless and 410 nm for the Bluephase G2.

Transmitted Radiant Exposure

Descriptive data analysis for radiant exposure values transmitted through various thicknesses of composite are shown in Table 3. For the Bluephase G2, no significant differences were found between the overall radiant exposures transmitted through the composites containing CQ or TPO (p=0.95, df=1, F=0.01). However, significant differences were not found between radiant exposures transmitted through the composites over different wavelength ranges for this curing light (p<0.04, df=1, F=4.98 and p<0.01, df=1, F=55.84, respectively). The radiant exposure transmitted through the composite containing TPO was higher than through the composite containing CQ over 420-495 nm at depths of 2 and 3 mm. In addition, the radiant exposure transmitted through the composite containing CQ was higher than through the composite containing TPO over 380-420 nm at depths of 1 and 2 mm.

For the VALO Cordless, significant differences were observed between the overall radiant exposures transmitted through the composites containing CQ and TPO (p<0.04, df=1, F=12.41). At 1-mm depth, a higher overall transmitted radiant exposure was found for the composite containing CQ when compared with the composite containing TPO. However, no differences were found at greater depths.

At depths of 1 and 2 mm, the radiant exposure values using Bluephase G2 light were significantly greater than those from the VALO Cordless for the wavelength region between 380 and 420 nm and between 420 and 495 nm for both photoinitiator types. However, there was no significant difference between lights at similar depths within the same photoinitiator system.

DC Profiles

Figure 6 illustrates the curing profiles of the composites containing CQ and TPO according to the different LED emittance regions (380-420 nm, 420-495 nm, and the overlap in between). A descriptive analysis is also shown in Table 4. As can be observed, no significant differences in DC were found between composites photoactivated by either of the two multiwave LEDs (p=0.89, df=12, F=0.52), and similar effects were found according to

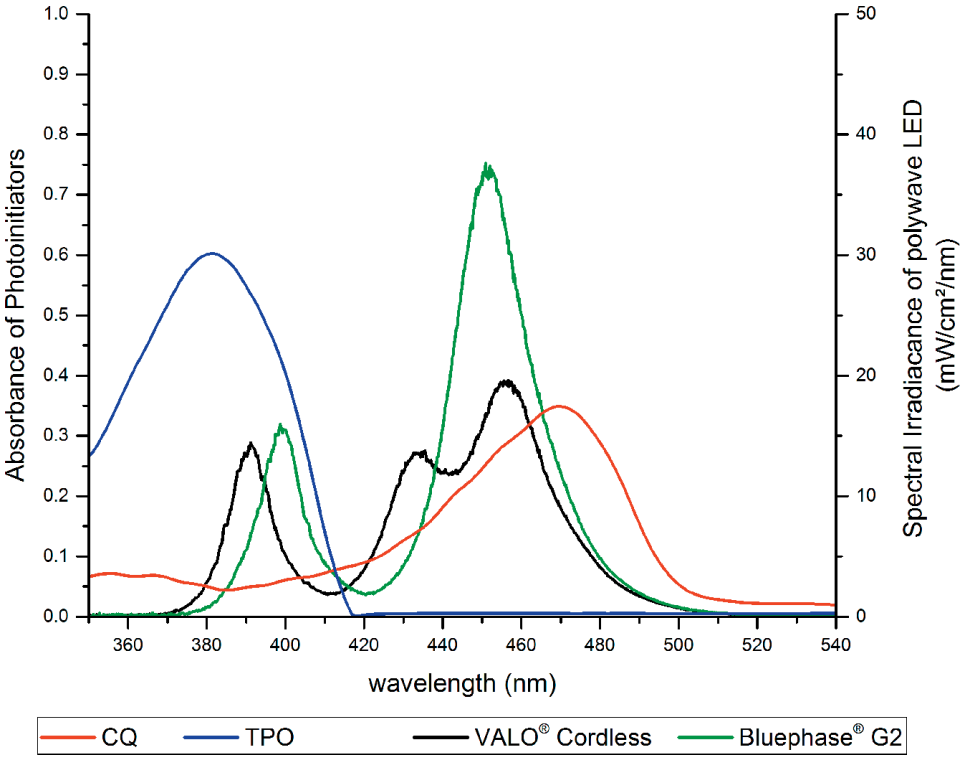

Figure 5. *Absolute irradiance (mW/cm²/nm) × wavelength (nm) for the two multiwave LEDs compared with the spectral absorbance profiles of CQ and TPO.*

the different LED emittance regions (p=0.09, df=5, F=2.11). When considering up to 1 mm in depth, no significant differences in DC were found between the photoinitiators. When evaluating the specimens starting at 2 mm in depth, the composite containing TPO showed a decrease in DC under the 420-495 nm emittance region, while the composite containing CQ showed similar cure efficiency decrease only at 3-mm depth, under both 380-420 nm and 420-495 nm emittance regions.

DISCUSSION

The first research hypothesis, that the beam profile of multiwave LEDs with different light emission tip types would be visually distinctly different, could not be rejected. The beam profile images illustrated in Figure 3 show that, despite the presence of higher and lower irradiance areas, there is some measurable irradiance of both types of LEDs emitting 380-420 nm and 420-495 nm wavelength ranges across the entire light tip of both multiwave LEDs.

Table 3: *Accumulated Radiant Exposure (J/cm²) Transmitted Through Each Resin-Based Composite Containing Different Photoinitiators at Different Depths According to Each Multiwave LED and Wavelength Emission, Mean (±SD)*[a]

	Depth, mm	CQ		TPO	
		Bluephase G2	VALO Cordless	Bluephase G2	VALO Cordless
380-495 nm (overall)	1	4.03 (0.26) Aa	3.19 (0.13) Ab	3.59 (0.30) Aa	2.56 (0.12) Bb
	2	1.63 (0.23) Aa	1.13 (0.12) Ab	1.91 (0.10) Aa	1.24 (0.07) Ab
	3	0.75 (0.04) Aa	0.60 (0.05) Aa	0.94 (0.06) Aa	0.68 (0.06) Aa
420-495 nm (blue)	1	3.33 (0.22) Aa	2.67 (0.10) Ab	3.16 (0.22) Aa	2.25 (0.09) Bb
	2	1.40 (0.19) Ba	1.00 (0.10) Ab	1.80 (0.08) Aa	1.17 (0.06) Ab
	3	0.64 (0.04) Ba	0.53 (0.05) Aa	0.90 (0.06) Aa	0.66 (0.06) Aa
380-420 (violet)	1	0.70 (0.05) Aa	0.53 (0.03) Aa	0.43 (0.09) Ba	0.31 (0.03) Ba
	2	0.23 (0.04) Aa	0.13 (0.02) Aa	0.11 (0.02) Ba	0.07 (0.01) Aa
	3	0.11 (0.01) Aa	0.06 (0.01) Aa	0.04 (0.01) Aa	0.02 (0.01) Aa

[a] *Uppercase letters compare means between initiator (CQ or TPO); lowercase letters compare means between LCU Bluephase G2 or VALO Cordless.*

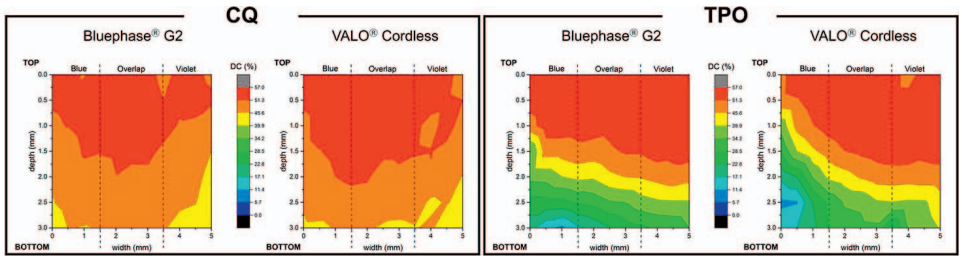

Figure 6. *Color-correlated curing profile of the mean DC (%) of CQ- and TPO-based composites according to the different LED emittance regions of the two multiwave LEDs.*

However, the highest irradiances are clearly localized near each respective LED chip emittances. Differences in the extent of light diffusion between the different wavelengths are expected because of the higher irradiance and quantity of the LED chips emitting 420-495 nm in comparison with the shorter wavelength at 380-420 nm,[12,18] as previously illustrated in Figure 1. However, these differences are also expected to be reduced according to the use of reflectors near the chip surfaces that are capable of mixing the light emittance from the different LED chips and light emission tip types that might be capable of homogenizing the light beam.

As a limitation of the method, the beam profile images are a projected light beam emitted from the curing light onto a diffusive, translucent glass surface. This type of target causes dispersion of the real beam output pattern. However, differences in the light diffusion extent between the two light beams from the different light emission tip types tested were still perceptible. Optical fiber bundles are only capable of mixing a multiwave beam when the individual fiber optics are not aligned (incoherent bundle), causing a scrambled beam output. Because the Bluephase G2 tip uses a coherent bundle, the aligned fiber optics are not capable of reducing the nonuniformity of the beam output. Thus, the fiber-optic arrangement merely transmits direct imaging of the LED array surface. However, it is important to point out that the new homogenizing fiber-optic tip from the Bluephase Style (Ivoclar Vivadent, Schaan, Liechtenstein) curing light now comes with a coherent assembly of optic fibers but also includes a thin diffusing film between the chip output and the actual entrance of the fibered bundle inside the guide, reducing the nonuniformity of the beam output in comparison with the older fiber-optic tips, such as the one from the Bluephase G2 that was used in this study.

The use of a digital single-lens reflex complementary metal-oxide semiconductor camera detector with a dynamic range of 49 dB, instead of a standard camera-based charge-coupled device beam profile system with a dynamic range over 64 dB, can reduce

Table 4: *Degree of Conversion (%; n=3) in Depth of Resin-Based Composites Containing Different Photoinitiators According to Each Multiwave LED and Wavelength Emission, Mean (±SD)*[a]

	Depth, mm	CQ		TPO	
		Bluephase G2	VALO Cordless	Bluephase G2	VALO Cordless
380-420 nm (blue)	0	52.4 (1.4) Aa	54.1 (1.3) Aa	55.4 (1.4) Aa	54.9 (2.6) Aa
	1	49.4 (0.9) ABa	52.9 (0.9) Aa	55.5 (0.9) Aa	55.8 (2.2) Aa
	2	47.0 (0.9) ABa	49.9 (2.0) Aa	47.6 (3.3) ABa	48.8 (5.0) ABa
	3	44.5 (1.2) Ba	41.0 (6.8) Ba	34.2 (14.9) Ba	40.3 (5.5) Ba
Overlap	0	52.5 (0.8) Aa	53.3 (1.4) Aa	55.7 (3.7) Aa	56.4 (0.7) Aa
	1	53.2 (0.4) Aa	54.8 (1.8) Aa	55.2 (3.7) Aa	55.8 (0.7) Aa
	2	50.5 (1.8) Aa	48.2 (4.4) ABa	45.7 (4.4) Aa	48.3 (0.7) Aa
	3	47.0 (0.1) Aa	44.4 (3.7) Ba	26.0 (7.3) Ba	32.9 (1.6) Ba
420-495 nm (violet)	0	52.7 (0.4) Aa	53.7 (1.0) Aa	54.8 (1.9) Aa	54.2 (1.3) Aa
	1	51.5 (1.2) ABa	53.7 (2.4) ABa	54.2 (3.1) ABa	51.0 (1.8) Aa
	2	49.5 (0.2) ABa	49.2 (1.9) ABa	39.9 (4.8) Ba	34.8 (4.3) Ba
	3	44.6 (2.3) Ba	44.5 (1.0) Ba	10.2 (5.3) Ca	21.1 (4.5) Ca

[a] *Within the photoinitiator type, lowercase letters compare means between columns (Bluephase G2 and VALO Cordless at same depth) and uppercase letters compare means between rows (depths 0, 1, 2, and 3 mm at same multiwave LED).*

the accuracy of the irradiance values shown on the beam profile images. However, all pixels were zeroed out using the minimum complementary metal-oxide semiconductor camera threshold; thus, all pixels are starting from the same baseline, reducing the lead to errors in the irradiance values shown in the beam profile images. Besides, even though a standard charge-coupled device camera-based beam profile can detect differences without pixel saturation up to 79,244.5 mW/cm^2 with an accuracy of 0.6 mW/cm^2, the camera used in this study had enough dynamic range and accuracy to detect differences in the irradiance emitted by the multiwave LEDs evaluated in this study. Specifically, when the camera used in this study camera was set to a minimum detection threshold of 50 mW/cm^2 for the characterization of the multiwave LEDs, the camera could detect differences without pixel saturation up to 14,091.9 mW/cm^2 with an accuracy of 3.5 mW/cm^2.

In contrast, the VALO Cordless uses a diffusive quartz glass lens (microlens) in an attempt to mix the light output wavelengths across the emitted beam. The explanation for this is the collimation of the light beam by the microlens that maintains the intensity across the nearly 10-mm diameter light tip from the VALO Cordless. However, the irradiance and the wavelengths from neither multiwave LEDs were uniformly distributed across the tip. As can be observed in Figure 3, even inside the black dashed square area of 5 × 5 mm that was used to represent the area of the light emission tip in which the specimens were exposed, the irradiation, irradiance, and wavelengths from neither multiwave LEDs were uniformly distributed.

The nonuniformity in the distribution of LED chips emitting different wavelengths can affect the extent of the curing efficiency of resin-based materials, depending on the type of photoinitiator system and duration of photoactivation.[10,18,19] A previous study showed that the nonuniform nature of the beam profile of a multiwave LED did not have an influence on the curing profile of resin-based composites, except for depth.[8] However, the decrease in DC with depth seems to be more related to the lower penetration of the violet light in comparison with the blue light, rather than to the nonuniformity in distribution of LED chips from multiwave LEDs. Still, that study used a minimum radiant exposure of 10 J/cm^2. Subsequently, the current experiment was performed using twice the radiant exposure values to check whether these differences would still occur with depth when using a higher radiant exposure rather than a minimum value.

As observed, similar effects were found according to the different LED emittance regions, when 24 J/cm^2 of radiant exposure was applied. Starting at 2 mm in depth, the composite containing TPO showed a decrease in DC under the 420-495 nm emittance region location, while the composite containing CQ showed no decrease in DC regardless of the emittance region. In addition, differences in light beam output from the various light emission tip types could not solve this problem. Thus, the second research hypothesis, that the nonuniform irradiance and wavelength emitted from multiwave LEDs would significantly reduce the DC in areas receiving lower irradiance and in which emissions fall outside of the absorbance range of the photoinitiator system, could not be rejected.

It is important to mention that exaggeration of monomer conversion is possible due to curing of unreacted monomers during the slicing process. However, using a water-cooled system, it is possible to overcome this issue. The IR thermal camera showed that the temperature increased up to 23.8°C during the cutting process, while the glass transition temperatures of the monomers used in the experimental composites are well above 100°C (BisGMA and BisEMA=110°C; UDMA=200°C; TEGDMA=170°C). Thus, no differences in monomer conversion would be expected using this method. Also, as explained before, the authors also used the FT-NIR for this test, rather than Raman, which would read only the surface of the specimen. FT-NIR readings were performed in the transmission mode rather than the reflection mode to evaluate DC in bulk rather than on the surface of the material, which reduces the influence of monomer elution from the surfaces of section specimens.

Despite the differences observed between beam profiles from both multiwave LEDs, no differences were found between the curing profiles provided by the two multiwave LEDs. Differences in the refractive indices between the resin matrix and filler particles leads to light scattering within resin-based composites, because of multiple reflections and refraction at the resin matrix and filler interfaces.[20,21] This light scattering within resin-based composites seems to effectively reduce the nonuniformity of the light output from the multiwave LEDs by scrambling the multiwave beam while being transmitted through the material, as observed in Figure 4. This finding would explain the uniformity of the curing profiles despite the nonuniformity of the multiwave beam outputs observed in Figure 3.

Another important aspect to be considered is the incidence of the light on the surface of the resin composite. For the optical fiber bundle, the output surface of the fiber is flat, and when it is placed in full contact with the sample, there is a mirroring image of the light output over the surface of the composite. However, for the microlens, this contact with the sample occurs only with the tangent of the microlens, so the light incidence on the surface of the sample comes from different directions, even though the convex aspect of the lens leads to a collimated light beam. This explains the better homogeneity of the beam profile through the composite for the VALO Cordless in comparison with the Bluephase G2.

However, despite generating a more homogeneous light beam through the composite, the differences in the light incidence create more reflection on the surface of the composite and reduce light transmittance through the composite when using the VALO cordless. On the other hand, for the Bluephase G2, there is a high probability of the light's reaching the surface of the composite at 90° with no or less scattering. This explains the higher radiant exposure transmittance for the Bluephase G2 in comparison with the VALO Cordless, as shown in Table 3, and the slightly better curing profile for the TPO-based composite when light cured with the Bluephase G2 rather than the VALO Cordless. However, it is important to point out that this study was conducted with the light tips placed perpendicular to the composite surface, and a different positioning would change the incidence of the light.[22] The curing light position is an example of a clinical aspect that might not often concern dentists. In fact, the curing light position can affect the amount of light delivered to the restoration.[23] Ideally, the curing light should be placed perpendicular to the composite surface; however, it is known that depending on the restoration location, the hand preference of the operator, or position on the side of the chair during the photoactivation process, this is not always possible or convenient and is possibly neglected by the operator.

Still, although the nonuniform light beam emitted from the two multiwave LEDs did not affect the curing profile of resin-based composites, light transmission within 380-420 nm seems to be reduced with depth, affecting the curing profile of composites containing photoinitiators with absorbance falling within this emission range. According to Rayleigh's scattering theory, it is expected that light transmission into deeper portions of a restoration might be reduced at shorter wavelengths.[20,21] Rayleigh scattering is the elastic scattering of electromagnetic radiation by particles much smaller than the wavelength of the radiation. This aspect means that when light travels through the matter, it tends to be scattered, and the amount of scattering is inversely proportional to the forth power of the wavelength of the radiation inside the visible spectrum. Thus, as the absorbance of TPO exclusively falls within a shorter wavelength emission (380-420 nm) in comparison with CQ (420-495 nm), the resultant increase in its scattering clearly imposes different limitations for depth of cure.

Differences in the degree of monomer conversion with depth, according to the type of photoinitiator and the LED emittance region, establishes the influence of the light beam of multiwave LEDs on the curing profile of resin-based composites containing different photoinitiators.[10,18,19] However, differences in photoinitiator and LED emittance regions do not necessarily influence the cure efficiency of the entire restoration.[10] As observed in the present study, the DC of CQ-based composites became affected starting at 3 mm in depth, which does not affect the conventional incremental restorative technique that uses 2-mm-thick layers. TPO-based composites, however, presented decreased DC at 2-mm depth located under the 420-495 nm emittance region, which is clearly related to the higher light-scattering extent of the shorter wavelengths through the composite depth.[20,24]

Thus, data in the present study demonstrate there were no differences between the curing profiles provided by the different multiwave LEDs. In addition, similar effects of the different LED emittance regions were found regardless of the different light emission tip types (microlens or coherent bundle). Many factors can influence light distribution through the resin-based composites, such as differences in the refractive indices of the resin matrix and filler content,[20,21] with it being difficult to predict the real effect of the beam profile on the curing profile of resin-based composites. However, within the limitations of this study, a standardized experimental resin-based composite containing the same resin matrix and filler content, but varying only in the type of photoinitiator, allowed the conclusion that, despite the nonuniform light beam emitted from the two multiwave LEDs being visually distinctly different, the curing profile of resin-based composites was not affected when higher radiant exposure values were used. However, it is important

to point out that light transmission within 380-420 nm is reduced with depth, directly affecting the curing profile of composites containing photoinitiators with absorbance falling within this emission range.

Moreover, there are still many unanswered questions about the influence of multiwave light beam profiles on the curing profile of resin materials. Further studies are needed to evaluate the influence of multiwave light beam profiles on the curing profile of bulk-fill resin-based composites with depth. Because bulk-fill materials are formulated to increase light transmittance and increase the depth of cure, it would be interesting to further explore the effect of wavelength-dependent scattering of these products. In addition, Class I restorations are approximately 5-mm wide. The current results demonstrate that, even inside the central area of 5 $\times$ 5 mm of the multiwave LED where the specimens were exposed to nonuniform irradiation, this nonuniformity is much more evident through the entire light tip. Thus, it would be interesting to further explore the influence of multiwave light beam profiles on the curing profile of much wider, Class II restorations.

CONCLUSIONS

Within the limitations of the current study, the following conclusions can be made:

1. Multiwave LEDs have a nonuniform irradiance and wavelength light beam emission, regardless of the light emission tip type used (microlens or coherent optical fiber bundle).
2. Despite the fact that the nonuniform light beam emitted from the two multiwave LEDs was visually distinctly different when delivering 24 J/cm^2, the curing profile of the model resin-based composite was not affected. However, light transmission within 380-420 nm seems to be reduced with depth, which directly affects the curing profile of composites containing photoinitiators, with absorbance falling within this emission range.

Acknowledgements

This study was supported by the FAPESP (grant 2013/04241-2 and grant 2014/03028-6). DO is a postdoctoral researcher at FAPESP (grant 2016/05823-3 and 2017/22161-7), and MR is a PhD researcher at FAPESP (grant 2016/06019-3 and 2017/22195-9). We would like to acknowledge Esstech and Evonik for the kind donation of the materials used in this study. We also acknowledge Dr Carmem Pfeifer for helping to develop the curing profile method used in this study.

Conflict of Interest

The authors of this article certify that they have no proprietary, financial, or other personal interest of any nature or kind in any product, service, and/or company that is presented in this article.

(Accepted 20 September 2018)

REFERENCES

1. Rueggeberg FA (2011) State-of-the-art: dental photocuring—a review *Dental Materials* **27(1)** 39-52. http://dx.doi.org/10.1016/j.dental.2010.10.021
2. Jandt KD & Mills RW (2013) A brief history of LED photopolymerization *Dental Materials* **29(6)** 605-617. http://dx.doi.org/10.1016/j.dental.2013.02.003
3. Labsphere I. (2015) *The Radiometry of Light Emitting Diodes—LEDs Technical Guide*. North Sutton, NH: Labsphere.
4. Shortall AC, Felix CJ, & Watts DC (2015) Robust spectrometer-based methods for characterizing radiant exitance of dental LED light curing units *Dental Materials* **31(4)** 339-350. http://dx.doi.org/10.1016/j.dental.2015.02.012
5. Leprince JG, Palin WM, Hadis MA, Devaux J, & Leloup G (2013) Progress in dimethacrylate-based dental composite technology and curing efficiency *Dental Materials* **29(2)** 139-156. http://dx.doi.org/10.1016/j.dental.2012.11.005
6. de Oliveira DC, Rocha MG, Gatti A, Correr AB, Ferracane JL, & Sinhoret MA (2015) Effect of different photoinitiators and reducing agents on cure efficiency and color stability of resin-based composites using different LED wavelengths *Journal of Dentistry* **43(12)** 1565-1572. http://dx.doi.org/10.1016/j.dent.2015.08.015
7. Alvim HH, Alecio AC, Vasconcellos WA, Furlan M, de Oliveira JE, & Saad JR (2007) Analysis of camphorquinone in composite resins as a function of shade *Dental Materials* **23(10)** 1245-1249.
8. de Oliveira DC, Rocha MG, Correr IC, Correr AB, Ferracane JL, & Sinhoreti MA (2016) The effect of combining photoinitiator systems on the color and curing profile of resin-based composites *Dental Materials* **32(10)** 1209-1217. http://dx.doi.org/10.1016/j.dental.2016.06.010
9. Salgado VE, Albuquerque PP, Cavalcante LM, Pfeifer CS, Moraes RR, & Schneider LF (2014) Influence of photoinitiator system and nanofiller size on the optical properties and cure efficiency of model composites *Dental Materials* **30(10)** e264-e271. http://dx.doi.org/10.1016/j.dental.2014.05.019
10. Li X, Pongprueksa P, Van Meerbeek B, & De Munck J (2015) Curing profile of bulk-fill resin-based composites *Journal of Dentistry* **43(6)** 664-672. http://dx.doi.org/10.1016/j.dent.2015.01.002
11. Price RB, Rueggeberg FA, Labrie D, & Felix CM (2010) Irradiance uniformity and distribution from dental light curing units *Journal of Esthetic and Restorative Dentistry* **22(2)** 86-101. http://dx.doi.org/10.1111/j.1708-8240.2010.00318.x
12. Michaud PL, Price RB, Labrie D, Rueggeberg FA, & Sullivan B (2014) Localised irradiance distribution found

in dental light curing units *Journal of Dentistry* **42(2)** 129-139. http://dx.doi.org/10.1016/j.dent.2013.11.014

13. Schreiber P, Kudaev S, Dannberg P, & Zeitner UD (2005) Homogeneous LED-illumination using microlens arrays *Proceedings* of *SPIE* **5942(1)** 1-9. http://dx.doi.org/10.1117/12.618747
14. Ghatak A & Thyagarajan K (2008) Optical waveguides and fibers In: Roychoudhuri C (ed) Fundamentals of photonics *SPIE Digital Library* **TT79** 249-292. https://spie.org/Documents/Publications/00%20STEP%20Module%2007.pdf
15. Schneider LF, Cavalcante LM, Consani S, & Ferracane JL (2009) Effect of co-initiator ratio on the polymer properties of experimental resin composites formulated with camphorquinone and phenyl-propanedione *Dental Materials* **25(3)** 369-375. http://dx.doi.org/10.1016/j.dental.2008.08.003
16. Rueggeberg FA, Hashinger DT, & Fairhurst CW (1990) Calibration of FTIR conversion analysis of contemporary dental resin composites *Dental Materials* **6(4)** 241-249.
17. Schindelin J, Arganda-Carreras I, Frise E, Kaynig V, Longair M, Pietzsch T, Preibisch S, Rueden C, Saalfeld S, Schmid B, Tinevez JY, White DJ, Hartenstein V, Eliceiri K, Tomancak P, & Cardona A (2012) Fiji: an open-source platform for biological-image analysis *Nature Methods* **9** 676-682. http://dx.doi.org/10.1038/nmeth.2019
18. Price RB, Labrie D, Rueggeberg FA, Sullivan B, Kostylev I, & Fahey J (2014) Correlation between the beam profile from a curing light and the microhardness of four resins *Dental Materials* **30(12)** 1345-1357.
19. Haenel T, Hausnerova B, Steinhaus J, Price RB, Sullivan B, & Moeginger B (2015) Effect of the irradiance distribution from light curing units on the local microhardness of the surface of dental resins *Dental Materials* **31(2)** 93-104. http://dx.doi.org/10.1016/j.dental.2014.11.003
20. dos Santos GB, Alto RV, Filho HR, da Silva EM, & Fellows CE (2008) Light transmission on dental resin composites *Dental Materials* **24(5)** 571-576.
21. Shortall AC, Palin WM, & Burtscher P (2008) Refractive index mismatch and monomer reactivity influence composite curing depth *Journal of Dental Research* **87(1)** 84-88.
22. Andre CB, Nima G, Sebold M, Giannini M, & Price RB (2018) Stability of the light output, oral cavity tip accessibility in posterior region and emission spectrum of light-curing units. *Operative Dentistry* **43(4)** 398-407.
23. Soares CJ, Bragança GF, Pereira RADS, Rodrigues MP, Braga SSL, Oliveira LRS, Giannini M, & Price RB (2018) Irradiance and radiant exposures delivered by LED light-curing units used by a left and right-handed operator. *Brazilian Dental Journal* **29(3)** 282-289.
24. Harlow JE, Rueggeberg FA, Labrie D, Sullivan B, & Price RB (2016) Transmission of violet and blue light through conventional (layered) and bulk cured resin-based composites *Journal of Dentistry* **53** 44-50. http://dx.doi.org/10.1016/j.dent.2016.06.007